

## Table of Contents

<b>I. General</b> .....	<b>S2</b>
<b>II. Experimental details</b> .....	<b>S3</b>
<b>III. Association experiments</b> .....	<b>S7</b>
Job Plot.....	S7
NMR Binding Experiments.....	S7
<b>IV. Crystallographic details</b> .....	<b>S12</b>
<b>V. UV/Vis spectroscopy</b> .....	<b>S20</b>
<b>VI. References</b> .....	<b>S21</b>
<b>VII. <sup>1</sup>H, <sup>19</sup>F and <sup>13</sup>C NMR Spectra</b> .....	<b>S22</b>

## I. General

Solvents and starting materials were purchased from Sigma Aldrich, TCI, Fisher Scientific, Alfa Aesar or Carl Roth and used as received. Dry solvents were obtained from an MBRAUN solvent purification system. Reactions were monitored by thin layer chromatography (TLC) carried out on silica gel plates (ALUGRAM<sup>®</sup> Xtra SIL G/UV254, Macherey Nagel) using UV light for visualization. Column chromatography was carried out with silica gel (Silica 60 M, 0.04-0.063 mm, Macherey Nagel) using eluents as specified.

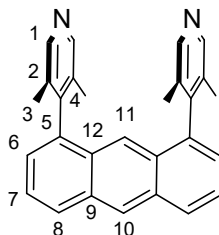
NMR spectra were recorded on a Bruker Avance III 300 and a Bruker Avance III 600 spectrometer at 25 °C using residual protonated solvent signals as internal standards for <sup>1</sup>H and <sup>13</sup>C spectra (<sup>1</sup>H:  $\delta(\text{CDCl}_3) = 7.26$  ppm,  $\delta(\text{C}_6\text{D}_6) = 7.16$  ppm,  $\delta(\text{CD}_3\text{CN}) = 1.94$  ppm ; <sup>13</sup>C:  $\delta(\text{CDCl}_3) = 77.16$  ppm,  $\delta(\text{C}_6\text{D}_6) = 128.06$  ppm,  $\delta(\text{CD}_3\text{CN}) = 118.26, 1.32$  ppm). Splitting patterns are abbreviated as follows: singlet (s), doublet (d), triplet (t), doublet of doublet (dd) and multiplet (m). Infrared spectra were recorded on a Jasco FT/IR-6200 and Shimadzu FT/IR IR Affinity-1 with an ATR attachment. Relative intensities of absorption bands are reported as s (strong), m (medium), w (weak) and br (broad). Electro-spray ionization high-resolution mass spectrometry was performed on a UHR-QTOF maXis 4G (Bruker Daltonics, Billerica, Massachusetts).

UV/vis spectroscopy was performed on a Perkin Elmer Lambda 19. A 405 nm LED (M405L3) and a 455 nm LED (M455L3), together with a LED driver (LEDD1B), from Thorlabs were applied for photoisomerization.

1,8-dichloroanthraquinone was used to prepare 1,8-dibromoanthraquinone.<sup>[1]</sup> Reducing 1,8-dibromoanthraquinone with aluminium in H<sub>2</sub>SO<sub>4</sub><sup>[2]</sup> followed by sodium borohydride addition<sup>[1]</sup> gave 1,8-dibromoanthracene. 1,8-Diiodo-9-mesitylanthracene was synthesized from 4,5-diiodo-9-anthrone<sup>[3]</sup> which was obtained from 1,8-dichloroanthraquinone by halide exchange<sup>[3,4]</sup> followed by reduction using sodium borohydride.<sup>[5]</sup> 3,5-Lutidine was used to prepare 3,5-lutidine-4-boronic acid pinacol ester by oxidation to the corresponding *N*-oxide, *para*-selective bromination, reduction followed by a bromine-lithium exchange and treatment with tributylborate and pinacol.<sup>[6-9]</sup> 4,4'-Diiodooctafluoroazobenzene (**A1**) was synthesized starting from 2,3,5,6-tetrafluoroaniline *via* 4-iodo-2,3,5,6-tetrafluoroaniline.<sup>[10]</sup> 2,6-Difluoro-4-iodoaniline, which was obtained by *para*-selective iodination of 2,6-difluoroaniline, was used to prepare 2,2',6,6'-tetrafluoro-4,4'-diiodoazobenzene (**A3**).<sup>[11]</sup>

## II. Experimental details

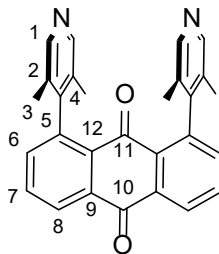
### 1,8-bis(3,5-dimethylpyridin-4-yl)anthracene (U1)



A Schlenk tube was charged with 1,8-dibromoanthraquinone (84.0 mg, 0.250 mmol, 1.0 eq.), 3,5-lutidine-4-boronic acid pinacol ester (141 mg, 0.600 mmol, 2.4 eq.),  $K_3PO_4$  (160 mg, 0.750 mmol, 3.0 eq.),  $Pd(OAc)_2$  (6.1 mg, 0.025 mmol, 10 mol%) and triphenylphosphine (30.0 mg, 0.115 mmol, 0.5 eq.). 0.5 mL water and 1.5 mL 1,4-dioxane were added and the suspension was refluxed under a nitrogen atmosphere for 72 hours. After cooling to room temperature, the mixture was diluted with 10 mL water and extracted with DCM (3\*50 mL). The combined organic phases were dried over  $MgSO_4$  and the solvent was removed under reduced pressure. The crude product was purified by column chromatography (DCM:MeOH 40:1 to 10:1). The compound (70.0 mg, 0.167 mmol, 67 %) was isolated as a light brown solid.

$^1H$ -NMR (600 MHz,  $CDCl_3$ ):  $\delta$  = 8.60 (s, 1H, H10), 8.27 (s, 4H, H1), 8.08 (d,  $J$  = 8.6 Hz, 2H, H8), 7.55 (dd,  $J$  = 8.5, 6.6 Hz, 2H, H7), 7.19 (s, 1H, H11), 7.18 (s, 2H, H6), 1.78 (s, 12H, H3);  $^{13}C\{^1H\}$ -NMR (151 MHz,  $CDCl_3$ ):  $\delta$  = 148.3 (C1), 147.0 (C4), 136.1 (C6), 132.0 (C5), 131.4 (C12), 129.3 (C2), 128.3 (C7), 127.7 (C11), 125.6 (C8), 125.6 (C10), 120.9 (C9), 16.8 (C3); IR (ATR):  $\tilde{\nu}_{max}$  = 2920 (w), 1584 (m), 1547 (w), 1449 (m), 1410 (m), 1379 (m), 1319 (m), 1279 (w), 1159 (m), 1086 (w), 1032 (w), 999 (w), 876 (s), 818 (w), 795 (m), 748 (s), 737 (s), 708 (w), 662 (m); HRMS (ESI)  $m/z$  calculated for  $C_{28}H_{25}N_2$   $[M+H]^+$  389.2012; found  $m/z$  389.2010.

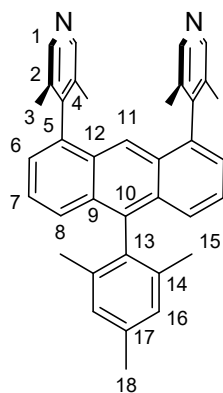
### 1,8-bis(3,5-dimethylpyridin-4-yl)anthracene-9,10-dione (U2)



A Schlenk tube was charged with 1,8-dibromoanthraquinone (92.0 mg, 0.250 mmol, 1.0 eq.), 3,5-lutidine-4-boronic acid pinacol ester (140 mg, 0.600 mmol, 2.4 eq.),  $K_3PO_4$  (159 mg, 0.750 mmol,

3.0 eq.), Pd(OAc)<sub>2</sub> (6.0 mg, 0.025 mmol, 10 mol%) and triphenylphosphine (30.0 mg, 0.115 mmol, 0.5 eq.). 0.5 mL water and 1.5 mL 1,4-dioxane were added and the suspension was refluxed under a nitrogen atmosphere for 72 hours. After cooling to room temperature, the mixture was diluted with 10 mL water and extracted with DCM (3\*50 mL). The combined organic phases were dried over MgSO<sub>4</sub> and the solvent was removed under reduced pressure. The crude product was purified by column chromatography (DCM:MeOH 40:1 to 10:1). The compound (70.0 mg, 0.167 mmol, 67 %) was isolated as a yellow solid. **<sup>1</sup>H-NMR** (600 MHz, CDCl<sub>3</sub>): δ = 8.43 (dd, *J* = 7.9, 1.3 Hz, 2H, H8), 8.22 (s, 4H, H1), 7.83 (dd, *J* = 7.6 Hz, 2H, H6), 7.30 (dd, *J* = 7.5, 1.3 Hz, 2H, H7), 1.80 (s, 12H, H3); **<sup>13</sup>C{<sup>1</sup>H}-NMR** (151 MHz, CDCl<sub>3</sub>): δ = 183.5 (C11), 182.8 (C10), 149.2 (C4), 148.2 (C1), 139.5 (C2), 136.3 (C6), 134.4 (C9), 133.9 (C7), 131.6 (C12), 129.1 (C5), 127.5 (C8), 17.2 (C3); **IR** (ATR):  $\tilde{\nu}_{max}$  = 3588 (w), 2941 (m), 1668 (s), 1574 (m), 1427 (m), 1410 (m), 1329 (s), 1283 (w), 1248 (s), 1161 (m), 1098 (m), 1076 (m), 1028 (w), 997 (w), 962 (m), 912 (m), 883 (m), 851 (m), 808 (s), 741 (s), 710 (m), 700 (m), 679 cm<sup>-1</sup> (m); **HRMS** (ESI) *m/z* calculated for C<sub>28</sub>H<sub>23</sub>N<sub>2</sub>O<sub>2</sub> [M+H]<sup>+</sup>: 419.1754; found *m/z* 419.1760.

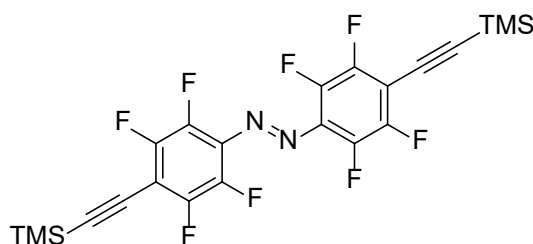
#### 4,4'-(10-mesitylanthracene-1,8-diyl)bis(3,5-dimethylpyridine) (U3)



A Schlenk tube was charged with 1,8-diiodo-10-mesitylanthracene (126 mg, 0.230 mmol, 1.0 eq.), 3,5-lutidine-4-boronic acid pinacol ester (161 mg, 0.690 mmol, 3.0 eq.), K<sub>3</sub>PO<sub>4</sub> (146 mg, 0.690 mmol, 3.0 eq.), Pd(OAc)<sub>2</sub> (5.0 mg, 0.023 mmol, 10 mol%) and triphenylphosphine (30.0 mg, 0.115 mmol, 0.5 eq.). 0.5 mL water and 1.5 mL 1,4-dioxane were added and the suspension was refluxed under a nitrogen atmosphere for 42 hours. 2.5 equivalents of the boronic acid ester were added again and the mixture was refluxed for additional 42 hours. After cooling to room temperature, the mixture was diluted with 5 mL water and extracted with DCM (3\*50 mL) and ethyl acetate (2\*50 mL). The combined organic phases were dried over MgSO<sub>4</sub> and the solvent was removed under reduced pressure. The crude product was purified by column chromatography (DCM:MeOH:TEA 10:1:0.1). The compound (49.0 mg, 0.097 mmol, 42 %) was isolated as a yellow solid.

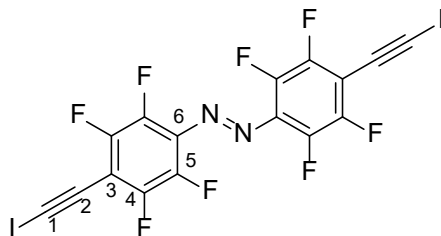
**<sup>1</sup>H-NMR** (600 MHz, CDCl<sub>3</sub>): δ = 8.28 (s, 4H, H1), 7.53 (d, *J* = 8.8 Hz, 2H, H8), 7.38 (dd, *J* = 8.8, 6.6 Hz, 2H, H7), 7.22 (s, 1H, H11), 7.15 (d, *J* = 6.6 Hz, 2H, H6), 7.13 (s, 2H, H16), 2.48 (s, 3H, H18), 1.81 (s, 12H, H3), 1.78 (s, 6H, H15); **<sup>13</sup>C{<sup>1</sup>H}-NMR** (151 MHz, CDCl<sub>3</sub>): δ = 148.3, 147.3, 137.6, 137.5, 137.2, 136.3, 134.5, 131.5, 130.0, 129.1, 128.5, 126.1, 125.6, 125.3, 120.4, 21.4, 20.2, 16.8; **IR** (ATR):  $\tilde{\nu}_{max}$  = 2966 (w), 2918 (m), 2854 (w), 2360 (s), 2337 (m), 1734 (m), 1585 (m), 1450 (m), 1414 (w), 1377 (w), 1276 (m), 1261 (w), 1166 (w), 826 (m), 748 (s), 706 cm<sup>-1</sup> (w); **HRMS** (ESI) *m/z* calculated for C<sub>37</sub>H<sub>35</sub>N<sub>2</sub> [M+H]<sup>+</sup> 507.2795; found *m/z* 507.2800.

### 1,2-bis(2,3,5,6-tetrafluoro-4-((trimethylsilyl)ethynyl)phenyl)diazene



A mixture of 1,2-bis(2,3,5,6-tetrafluoro-4-iodophenyl)diazene (130 mg, 0.225 mmol, 1.0 eq.), trimethylsilylacetylene (0.64 mL, 4.50 mmol, 20 eq.) and triethylamine (1.00 mL, 7.20 mmol, 32 eq.) was purged with nitrogen for 10 minutes. CuI (4.0 mg, 0.023 mmol, 10 mol%) and Pd(PPh<sub>3</sub>)Cl<sub>2</sub> (6.0 mg, 0.009 mmol, 4 mol%) were added and the mixture was refluxed for 5 hours. After cooling to room temperature, the mixture was diluted with 20 ml DCM and washed with 10 mL saturated aqueous NH<sub>4</sub>Cl solution. The aqueous phase was extracted with DCM and the combined organic layers were dried over Mg<sub>2</sub>SO<sub>4</sub> and filtrated over a small silica plug. The solvent was removed under reduced pressure yielding 83.0 mg (0.160 mmol, 71 %) of the crude product, which was used without further purification. **HRMS** (ESI) *m/z* calculated for C<sub>22</sub>H<sub>19</sub>F<sub>8</sub>N<sub>2</sub>Si<sub>2</sub> [M+H]<sup>+</sup> 519.0954; found *m/z* 519.0952.

### 1,2-bis(2,3,5,6-tetrafluoro-4-(iodoethynyl)phenyl)diazene (A2)



A solution of the previously synthesized 1,2-bis(2,3,5,6-tetrafluoro-4-((trimethylsilyl)ethynyl)phenyl)diazene (63.0 mg, 0.121 mmol, 1.0 eq.) in 15 mL acetonitrile was

degassed with N<sub>2</sub> for 10 minutes. AgF (34.0 mg, 0.267 mmol, 2.2 eq.) and NIS (60.0 mg, 0.267 mmol, 2.2 eq.) were added and the mixture was stirred at room temperature for 3 hours. The mixture was diluted with DCM (30 mL) and washed with saturated aqueous NH<sub>4</sub>Cl (20 mL). The aqueous layer was extracted with DCM (2x30 mL). The combined organic layers were dried over MgSO<sub>4</sub> and the solvent was removed under reduced pressure. The crude product was purified by column chromatography (CyHex:EE 95:5). The compound (0.025 mg, 0.040 mmol, 33 %) was isolated as red crystals.

**<sup>19</sup>F-NMR** (376 MHz, C<sub>6</sub>D<sub>6</sub>):  $\delta = E\text{-A2: } -137.17 - -137.50$  (m),  $-149.64 - -150.08$ ,  $Z\text{-A2: } -134.74 - -134.90$  (m),  $-147.96 - -148.10$  (m); **<sup>13</sup>C{<sup>1</sup>H}-NMR** (151 MHz, CDCl<sub>3</sub>):  $\delta = 148.5$  (d of m,  $J = 241$  Hz, C4),  $140.4$  (ddt,  $J = 262, 14, 4$  Hz, C5),  $132.6$  (m, C3 or C6),  $106.9$  (m, C3 or C6),  $79.2$  (t,  $J = 4$  Hz, C2),  $26.8$  (t,  $J = 4$  Hz, C1) **IR** (ATR):  $\tilde{\nu}_{max} = 2959$  (w),  $2923$  (m),  $2852$  (w),  $2179$  (w),  $1718$  (br),  $1481$  (s),  $1397$  (w),  $1260$  (m),  $1083$  (m),  $989$  (s),  $797$  (m); **HRMS** (ESI)  $m/z$  calculated for C<sub>16</sub>HF<sub>8</sub>I<sub>2</sub>N<sub>2</sub> [M+H]<sup>+</sup> 626.8096; found  $m/z$  626.8102.

### III. Association experiments

The constant component is referred to as “host” while the varied compound is called “guest”. Due to the lower solubility the XB acceptor was chosen as the host. NMR-spectra were recorded on a 600 MHz Bruker Avance III at 283 K. Chemical shifts are reported relative to the residual protonated solvent signal.

#### Job’s Plot

The method of continuous variation was applied to determine the stoichiometry of the formed boxes. Stock solutions of **A2** ( $c = 4.655$  mmol/L) and **U3** in benzene- $d_6$  were used to prepare samples containing the host in different mole fractions. The observed difference in chemical shift multiplied with the mole fraction of the host against the mole fraction of the host results in a parable with the maxima at 0.5 for a 1:1 or 2:2 complex.

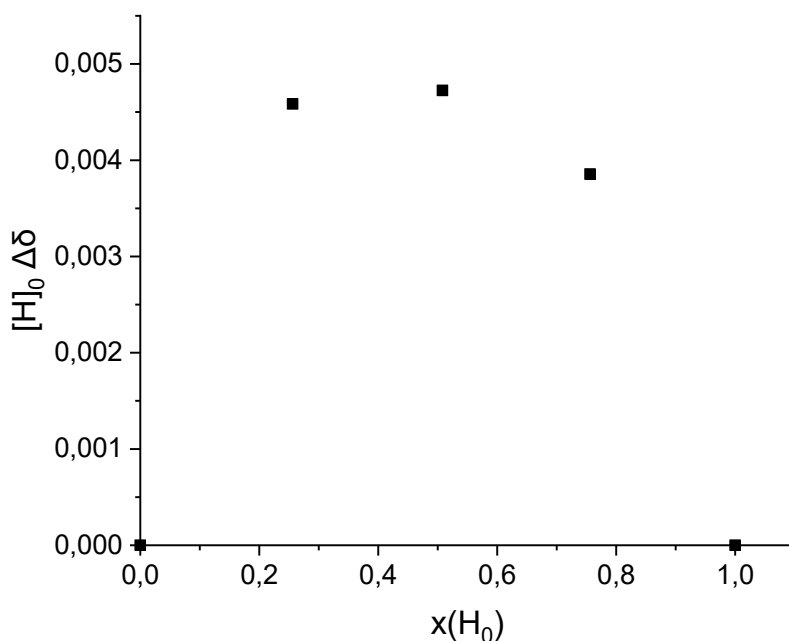
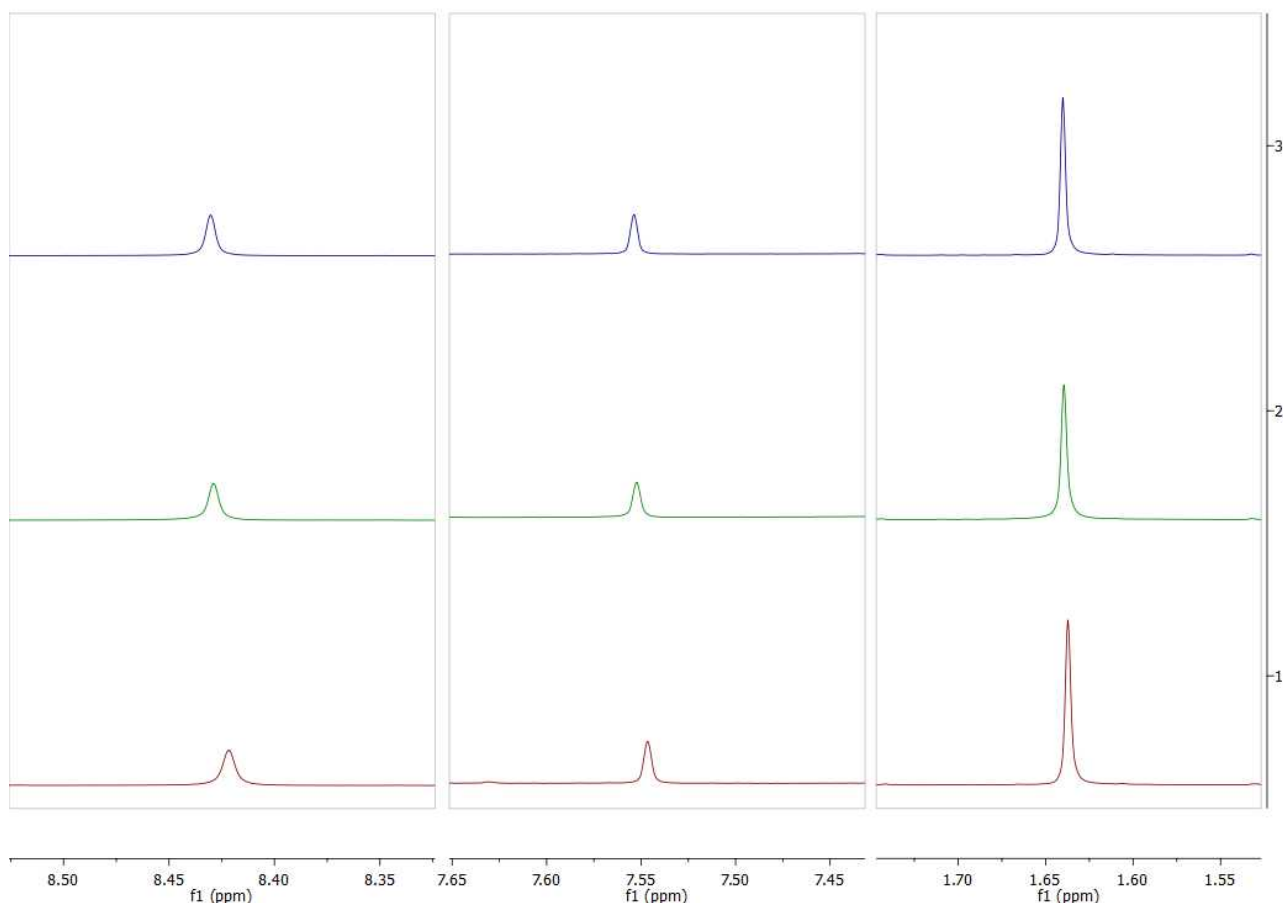


Figure S1. Job’s Plot of the complexation of **U3** and **A2**.

#### NMR Binding Experiments

Solutions of the host **U3** ( $c = 2.00$  mmol/L) and both azobenzenes in  $C_6D_6$  ( $c(\mathbf{A1}) = 11.4$  mmol/L and  $c(\mathbf{A2}) = 13.9$  mmol/L) were prepared, using only gravimetric analyses, and used as parent solutions to prepare samples containing 1:1 mixtures of host and guest. The measured spectra (Figure S.2) were used to estimate which of the synthesized azo compounds shows higher association tendencies.



**Figure S2.**  $^1\text{H-NMR}$  spectra of **U3** (blue), 1:1 mixtures of **U3**...**A1** (green) and **U3**...**A2** (red) at 283 K.

Solutions of the host **U3** ( $c = 2.17$  mmol/L) and guest **A2** ( $c = 39.05$  mmol/L) in  $\text{C}_6\text{D}_6$  were prepared using only gravimetric analyses. The guest solution was successively added to the host solution. Using OriginPro 2018b the graphs of the change of the chemical shift  $\Delta\delta$  against the guest concentration  $[G]_0$  were curve fitted using the orthogonal distance regression iteration algorithm. The following equation was used for curve fitting<sup>[12]</sup>:

$$\Delta\delta = \frac{\Delta\delta_{sat}}{2} \left[ \left( \frac{[G]_0}{[H]_0} + 1 + \frac{1}{K_a[H]_0} \right) - \sqrt{\left( \frac{[G]_0}{[H]_0} + 1 + \frac{1}{k_a[H]_0} \right)^2 - 4 \frac{[G]_0}{[H]_0}} \right]$$

The total concentration of the host  $[H]_0$  is constant while the total concentration of the guest  $[G]_0$  is varied. The association constant  $K_a$  and the change in chemical shift for a saturated system are obtained by curve fitting.

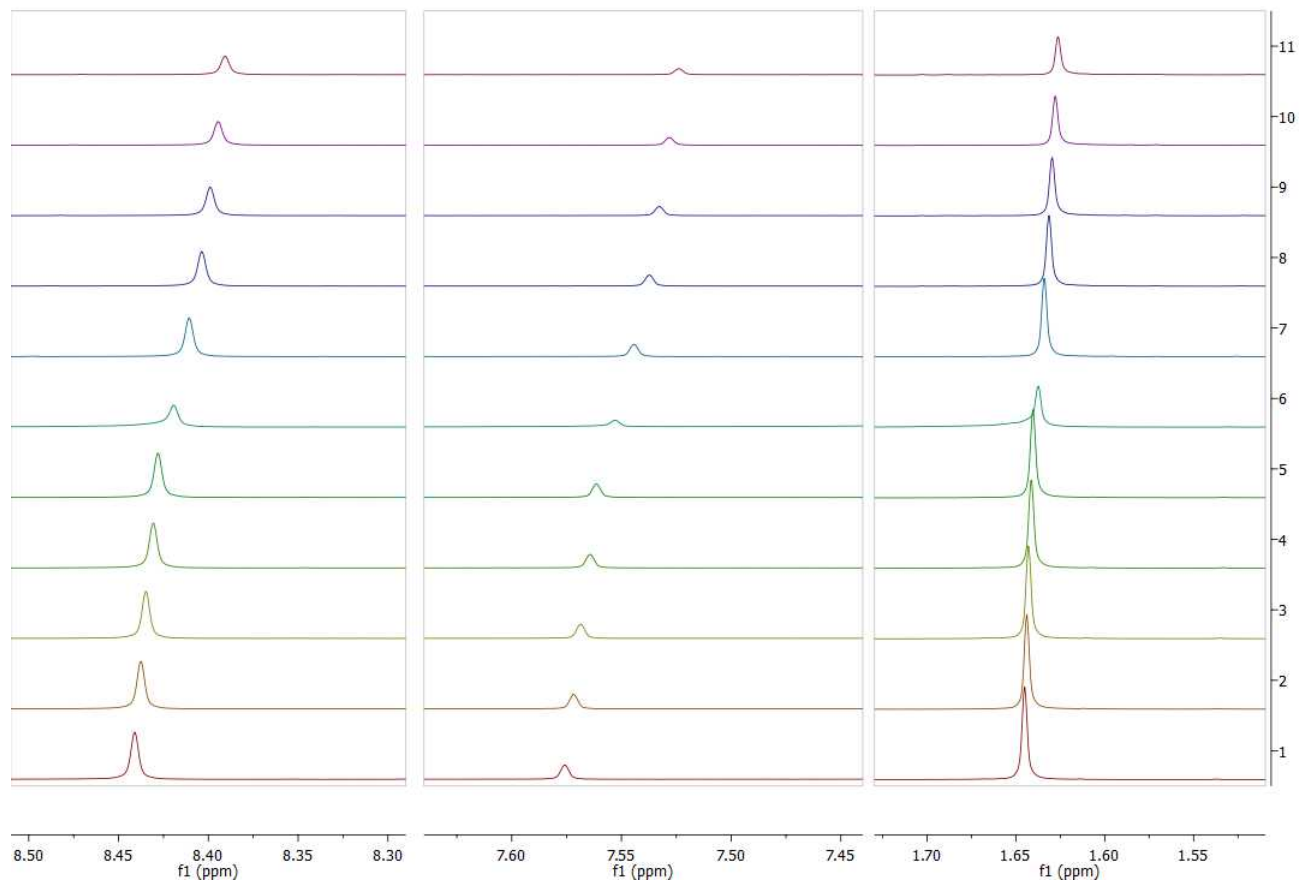
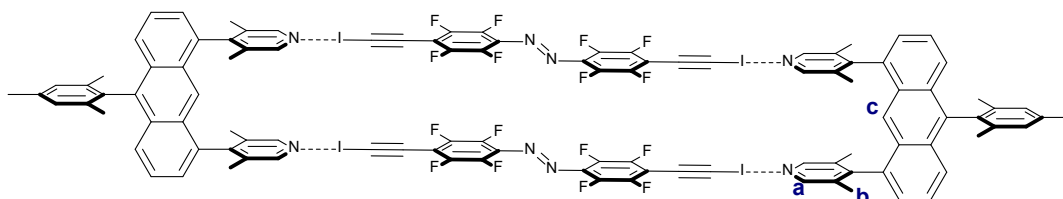


**Figure S3.**  $^1\text{H-NMR}$  binding titration progress in  $\text{C}_6\text{D}_6$  at 283 K. Displayed are the chemical shifts of the protons a (left), c (middle) and b (right). The shifts of a were used for the determination of  $K_a$ .

**Table S1:** Titration data of complexation derived from  $^1\text{H-NMR}$  binding titration (600 MHz). The concentration of the guest was varied while the concentration of the host ( $c_0 = 2.17 \text{ mmol/L}$ ) was maintained constant.

[A2]	$\Delta\delta$
mol/L	ppm
0,000E+00	0,0000
5,415E-04	0,0034
1,080E-03	0,0062
1,620E-03	0,0103
2,170E-03	0,0129
4,330E-03	0,0217
6,490E-03	0,0303
8,650E-03	0,0373
1,082E-02	0,0420
1,299E-02	0,0464
1,516E-02	0,0503

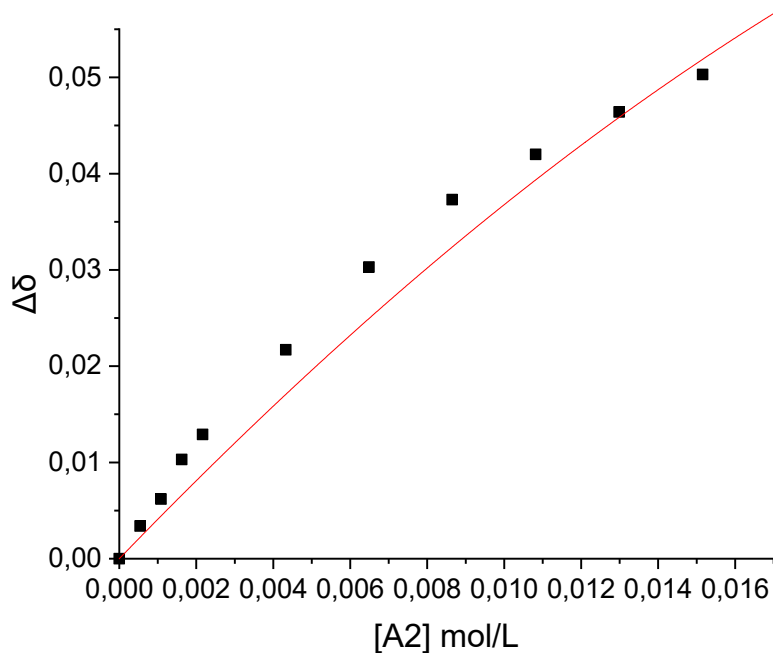


**Figure S4.**  $^1\text{H-NMR}$  binding titration of **U3** with **A2**. The change of the chemical shift of the lutidine proton a is plotted against the concentration of **A2** and fitted to a 1:1 isotherm. Determined  $K_a = 94 \text{ M}^{-1}$

Common errors taken into account for the titration results are attributed to inaccurate temperature measurement inside of the NMR during the measurements, gravimetric errors while preparing the stock solutions and NMR data processing (such as peak picking). Due to difficulties fitting the obtained data, although an  $r^2$  value of 0.997 was obtained, we decided to report binding as very low or unspecific, as indicated by  $K_a < 10^2 \text{ M}^{-1}$  in the main manuscript.

## IV. Crystallographic details

Single-crystals were mounted using a microfabricated polymer film crystal-mounting tool (dual-thickness MicroMount, MiTeGen) using low viscosity oil (perfluoropolyalkylether; viscosity 1800 cSt, ABCR) to reduce the X-ray absorption and scattering. A Bruker D8 Venture single-crystal X-ray diffractometer with area detector using Mo- $K_{\alpha}$  ( $\lambda = 0.71073 \text{ \AA}$ ) or Cu- $K_{\alpha}$  ( $\lambda = 1.54178 \text{ \AA}$ ) radiation was used for data collection at the temperature stated for each compound. Multiscan absorption corrections implemented in SADABS<sup>[13]</sup> were applied to the data. The structures were solved by intrinsic phasing (SHELXT-2013)<sup>[14]</sup> and refined by full-matrix least-squares methods on  $F^2$  (SHELXL-2014).<sup>[15]</sup> The hydrogen atoms were placed at calculated positions and refined by using a riding model. CCDC 1909803 (U1...A1), 1909801 (U1...A2), 1909802 (U2...A1) and 1909804 (A3) contain the supplementary crystallographic data for this paper. These data can be obtained free of charge from The Cambridge Crystallographic Data Centre.

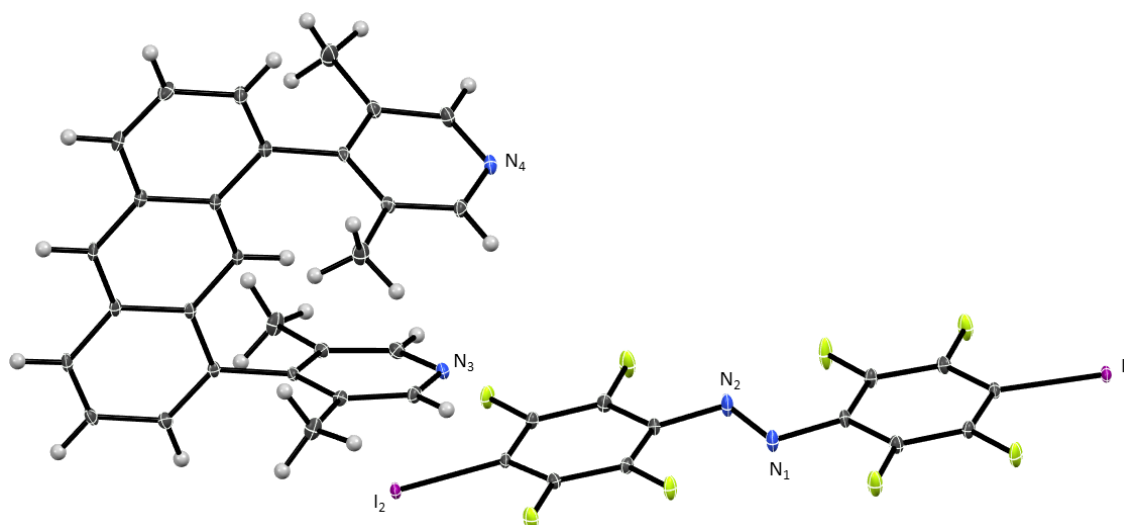


**Figure S5.** Single-crystal X-ray data of U1...A1 showing the asymmetric unit with thermal ellipsoids set at 50% probability. The structure was measured at 100 K and solved in the monoclinic space group  $P2_1/n$  with  $R_{\text{int}} = 0.0482$ ,  $R_1 = 0.0196$  and  $wR_2 = 0.0462$ . Selected bond lengths [ $\text{\AA}$ ]: I1–N4 2.784(2), I2–N3 2.756(1), N1–N2 1.234(2). The structure shows C–H...F contacts such as F1...H36 2.65, F6...H18C 2.75, F7...H13 2.55 and F7...H39B 2.66.

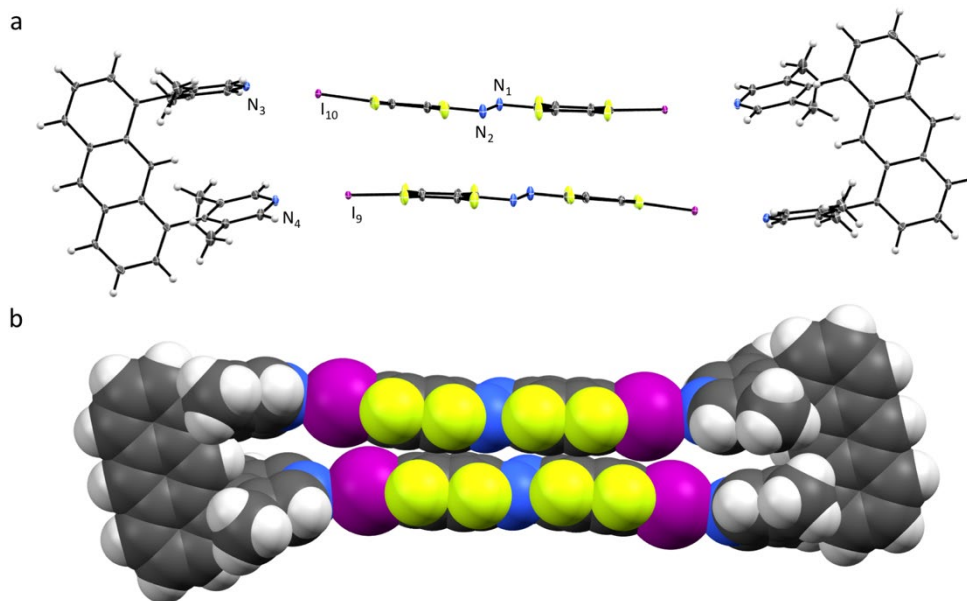


**Figure S6.** Single-crystal X-ray data of **U1...A1**, a) with thermal ellipsoids set at 50% probability and b) showing a space-filling model.

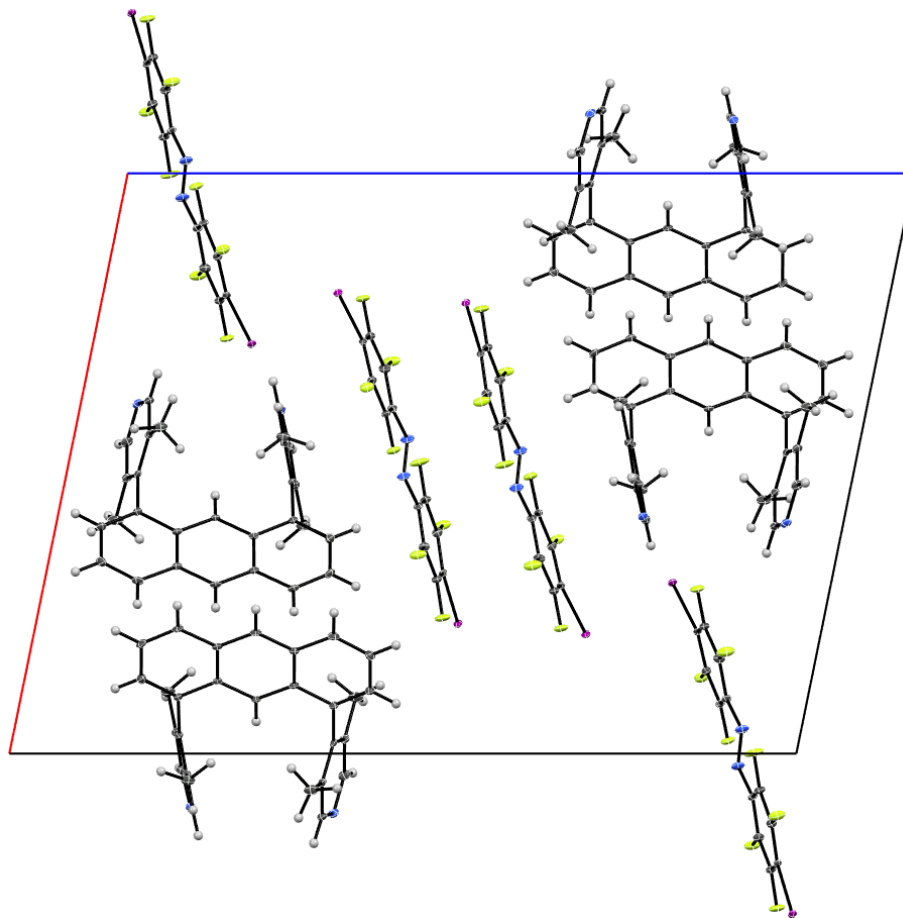


**Figure S7.** View of the unit cell of **U1...A1** along the crystallographic *b* axis. The anthracene units engage in an infinite herringbone type arrangement, supported by CH... $\pi$  interactions in the range from 3.14–3.56 Å.

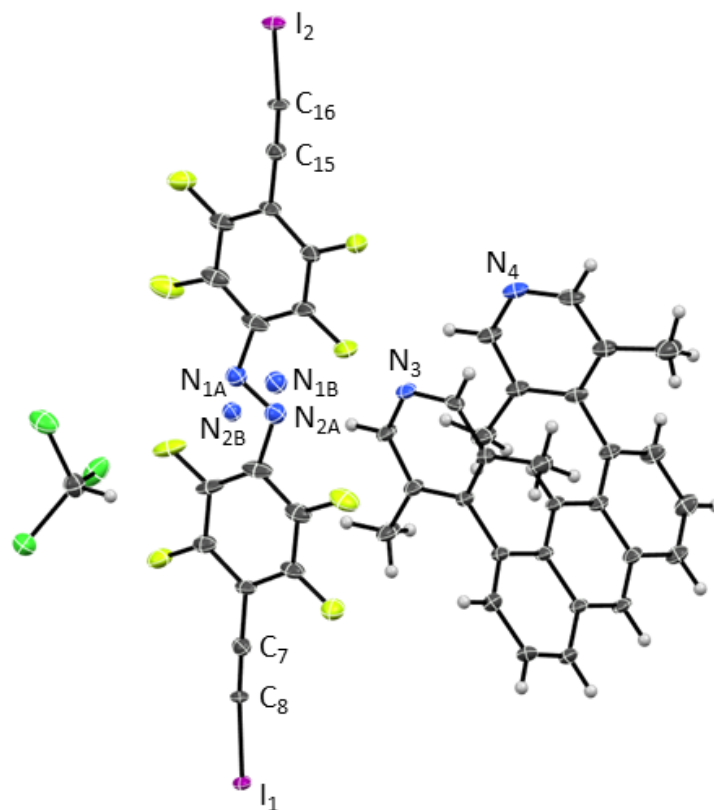


**Figure S8.** Single-crystal X-ray data of **U1...A2**, showing the asymmetric unit including the disorder of the azo bond and one ordered chloroform molecule with thermal ellipsoids set at 50% probability. The structure was measured at 122 K and solved in the triclinic space group P-1 with  $R_{int} = 0.0597$ ,  $R_1 = 0.0361$  and  $wR_2 = 0.0967$ . Selected bond lengths [ $\text{\AA}$ ]: I1–N3 2.726(3), I2–N4 2.835(3), C7–C8 1.193(5), C15–C16 1.180(5).

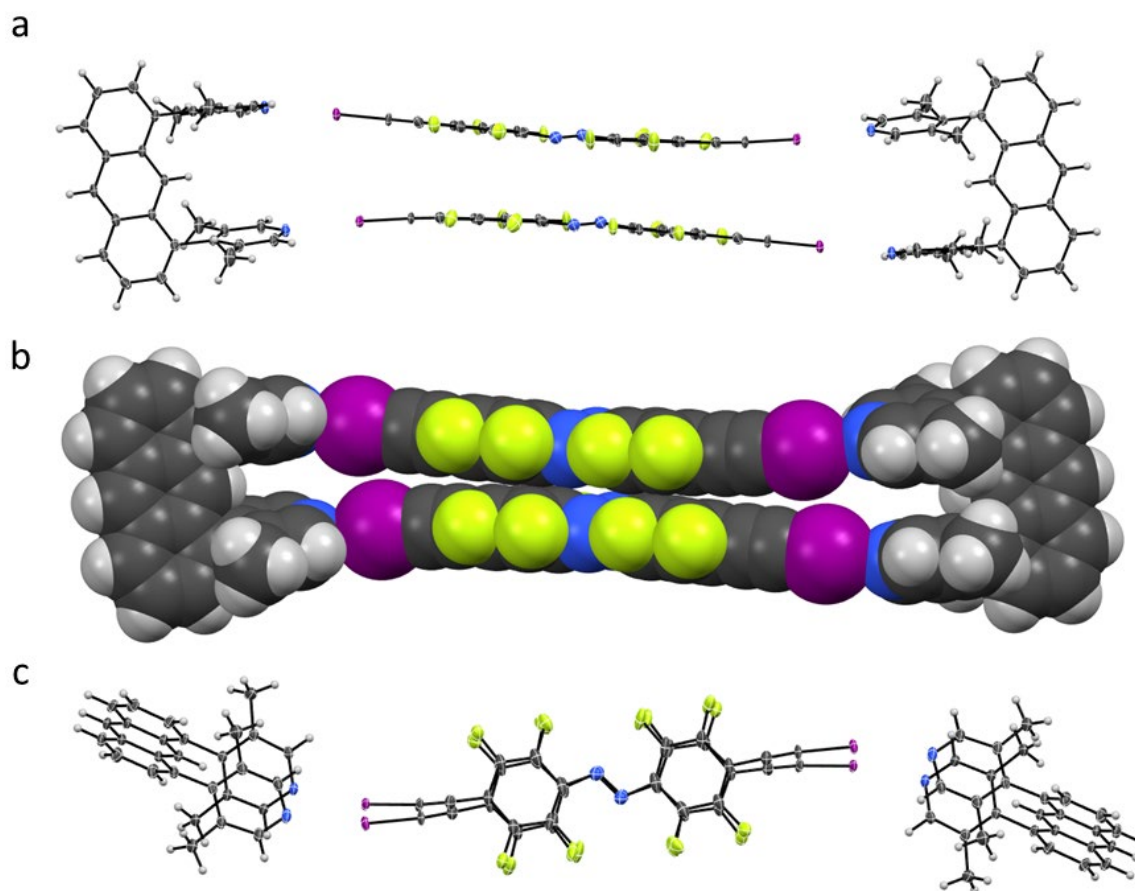


**Figure S9.** Single-crystal X-ray data of U1...A2, a) with thermal ellipsoids set at 50% probability, b) showing a space-filling model and c) showing the waviness of the box from above. Chloroform molecules and azobenzene disorder omitted for clarity.

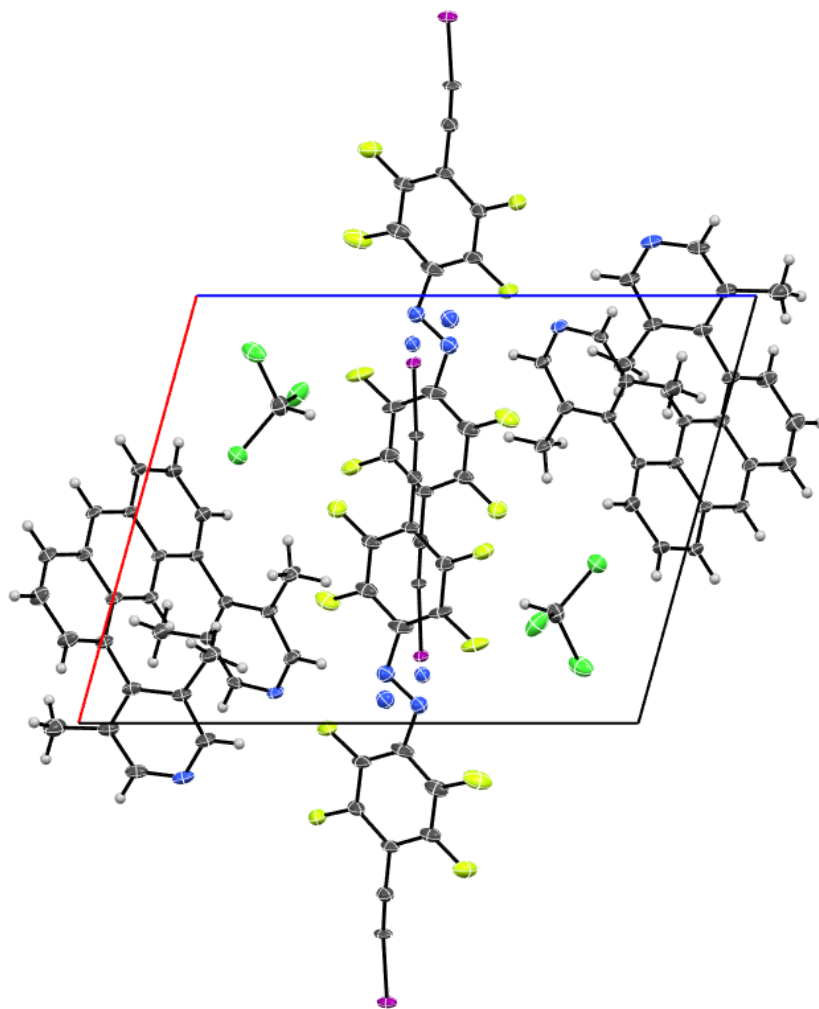


**Figure S10.** View of the unit cell of U1...A2 along the crystallographic *b* axis. The anthracene units interact loosely by forming head-to-tail dimers with centroid-to-centroid distances of 4.24–4.34 Å.

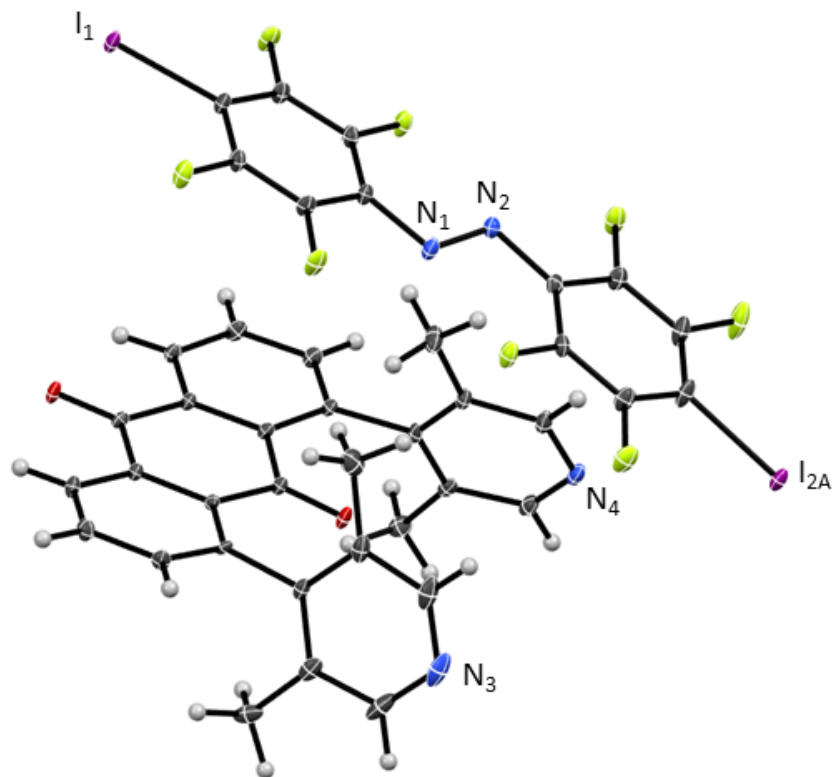


**Figure S11.** Single-crystal X-ray data of  $U2 \cdots A1$ , a) with thermal ellipsoids set at 50% probability and b) showing a space-filling model. The structure was measured at 100 K and solved in the triclinic space group P-1 with  $R_{int} = 0.0361$ ,  $R_1 = 0.0353$  and  $wR_2 = 0.0770$ . Selected bond lengths [ $\text{\AA}$ ]: I1–N4 2.764(3), I2A–N3 2.777(5), N1–N2 1.256(5).

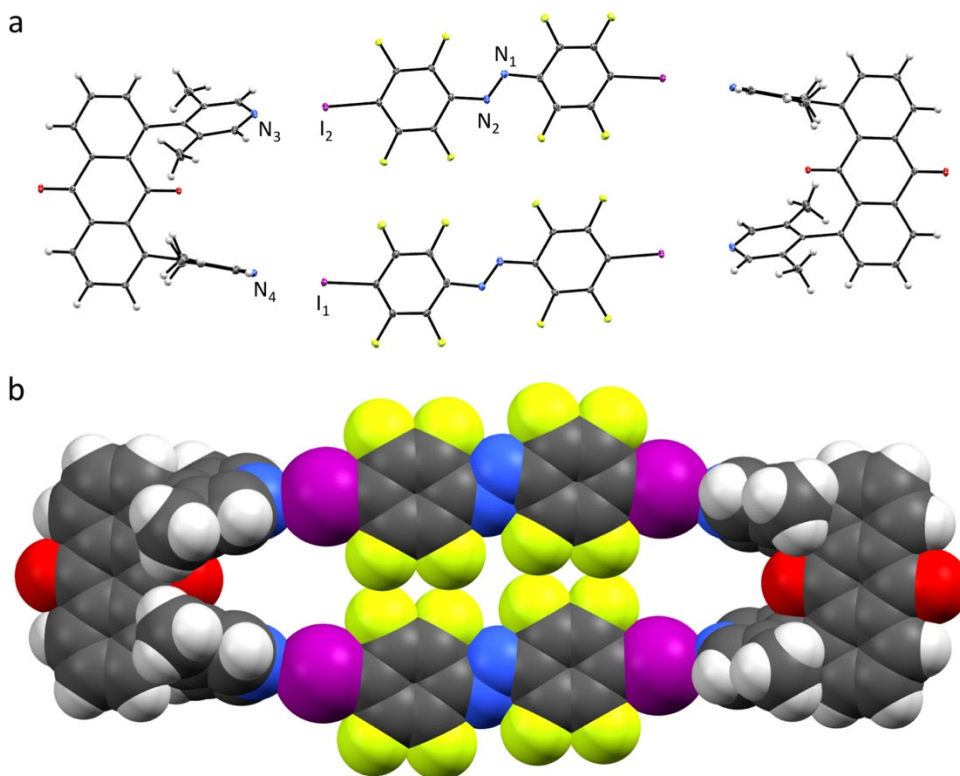


**Figure S12.** Single-crystal X-ray data of  $U2 \cdots A1$ , a) with thermal ellipsoids set at 50% probability and b) showing a space-filling model.

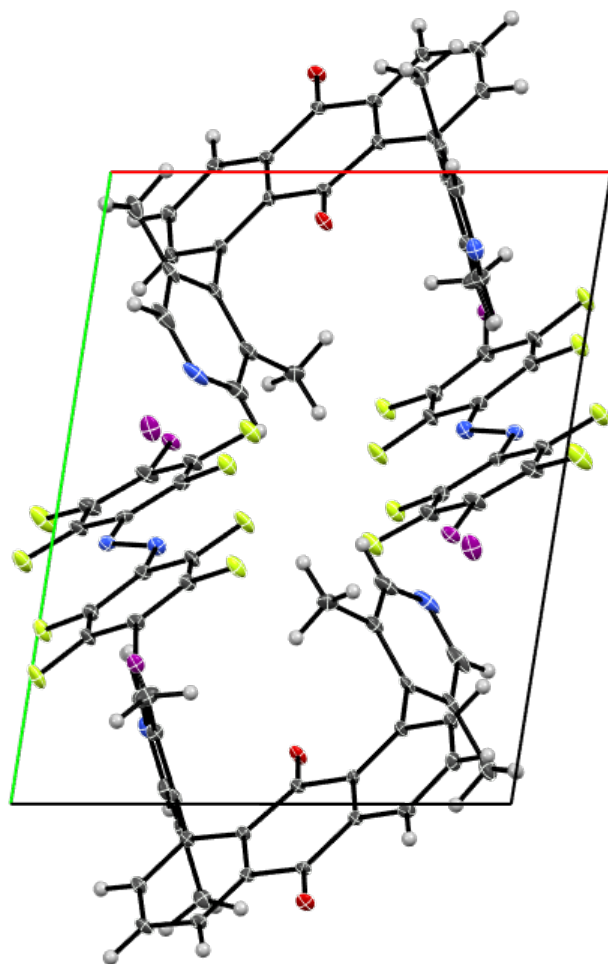


**Figure S13.** View of the unit cell of **U2...A1** along the crystallographic *b* axis. The anthracinone units show very loose dimer formation by off-set stacking with centroid-to-centroid distances of 4.04–4.19 Å.

Equimolar amounts of **U2** and **A3** were dissolved in acetonitrile. After slow evaporation of the solvent over a few days at room temperature, crystals suitable for single-crystal X-ray analysis were obtained of the azobenzene **A3** in form of orange needles together with colorless blocks of an acetonitrile solvate of **U2** in an attempt to prepare the supramolecular box **U2**·**A3**, which does not form under given conditions. The crystal structure of **A3** is reported below.

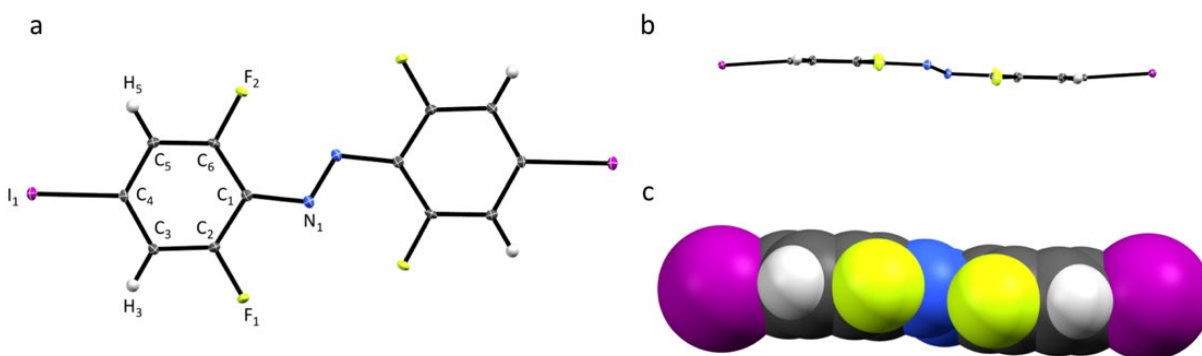


**Figure S14.** Single-crystal X-ray data of **A3**, a) and b) with thermal ellipsoids set at 50% probability and c) showing a space-filling model. The structure was measured at 100 K and solved in the monoclinic space group  $P2_1/c$  with half of the molecule in the asymmetric unit and  $R_{\text{int}} = 0.0186$ ,  $R_1 = 0.0136$  and  $wR_2 = 0.0334$ . Selected bond lengths [ $\text{\AA}$ ]: I1–C4 2.092(2), N1–N1 1.252(2).

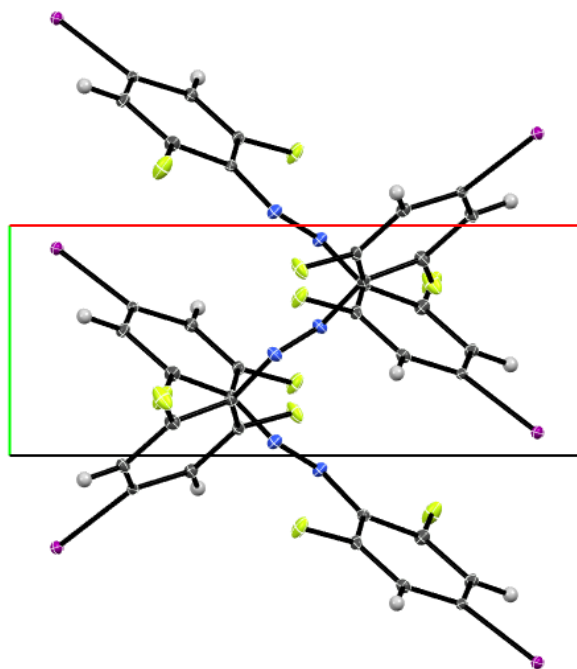


**Figure S15.** View of the unit cell of **A3** along the crystallographic  $c$  axis, showing the herringbone packing.

## V. UV/Vis spectroscopy

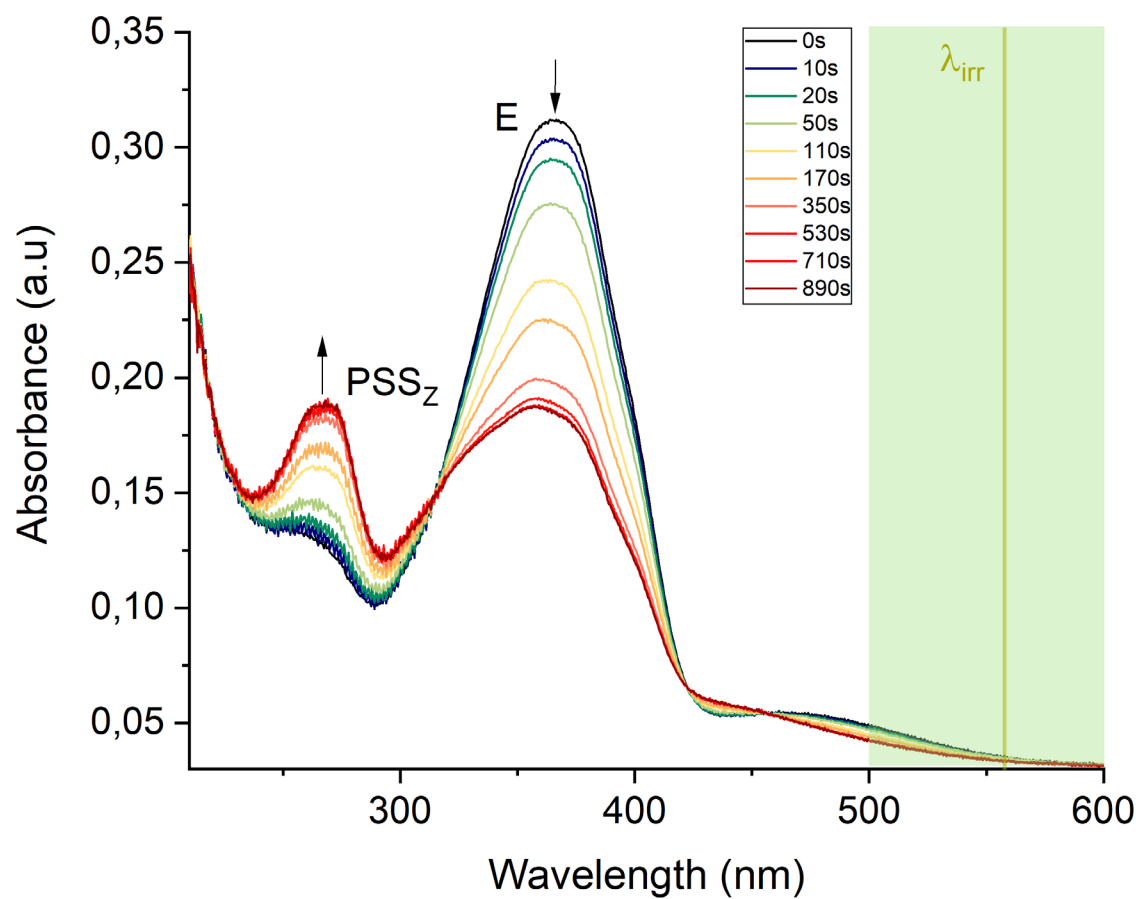


**Figure S16.** UV/Vis spectra of **A2** in acetonitrile ( $c = 7.67 \mu\text{mol/L}$ ) after irradiation with  $\lambda_{\text{irr}} = 565 \text{ nm}$ , as indicated by the green band. Irradiation times were determined using a stopwatch.

## VI. References

- [1] M. Pérez-Trujillo, I. Maestre, C. Jaime, A. Alvarez-Larena, J. Francesc Piniella and A. Virgili, *Tetrahedron Asymmetry*, 2005, **16**, 3084.
- [2] M. Yamashita, Y. Yamamoto, K. Akiba, D. Hashizume, F. Iwasaki, N. Takagi and S. Nagase, *J. Am. Chem. Soc.*, 2005, **127**, 4371.
- [3] M. Inoue, T. Iwanaga and S. Toyota, *Chem. Lett.*, 2013, **42**, 1499.
- [4] Y. Yang, J. Cui, Z. Li, K. Zhong, L. Y. Jin and M. Lee, *Macromolecules*, 2016, **49**, 5912.
- [5] M. Goichi, K. Segawa, S. Suzuki and S. Toyota, *Synthesis*, 2005, **13**, 2116.
- [6] S. Duric and C. C. Tzschucke, *Org. Lett.*, 2011, **13**, 2310.
- [7] P. Klán, *Monatsh. Chem.*, 1993, **124**, 327.
- [8] V. Diemer, H. Chaumeil, A. Defoin, A. Fort, A. Boeglin and C. Carré, *Eur. J. Org. Chem.*, 2008, **10**, 1767.
- [9] E. Ay, H. Chaumeil and A. Barsella, *Tetrahedron*, 2012, **68**, 628.
- [10] O. S. Bushuyev, A. Tomberg, T. Friščić and C. Barrett, *J. Am. Chem. Soc.*, 2013, **135**, 12556.
- [11] D. Bléger, J. Schwarz, A. M. Brouwer and S. Hecht, *J. Am. Chem. Soc.*, 2012, **134**, 20597.
- [12] K. Hirose, Quantitative Analysis of Binding Properties in *Analytical Methods in Supramolecular Chemistry* (Ed.: C. A. Schalley), Wiley-VCH, Weinheim, **2012**, 27-66.
- [13] G. M. Sheldrick, SADABS, program for empirical absorption correction of area detector data, University of Göttingen, Göttingen, 1996.
- [14] G. M. Sheldrick, SHELXT-2013, Program for Crystal Structure Solution, University of Göttingen, Göttingen, 2013.
- [15] G. M. Sheldrick, SHELXL-2014, Program for Crystal Structure Refinement, University of Göttingen, Göttingen, 2014.

## VII. $^1\text{H}$ , $^{19}\text{F}$ and $^{13}\text{C}$ NMR Spectra

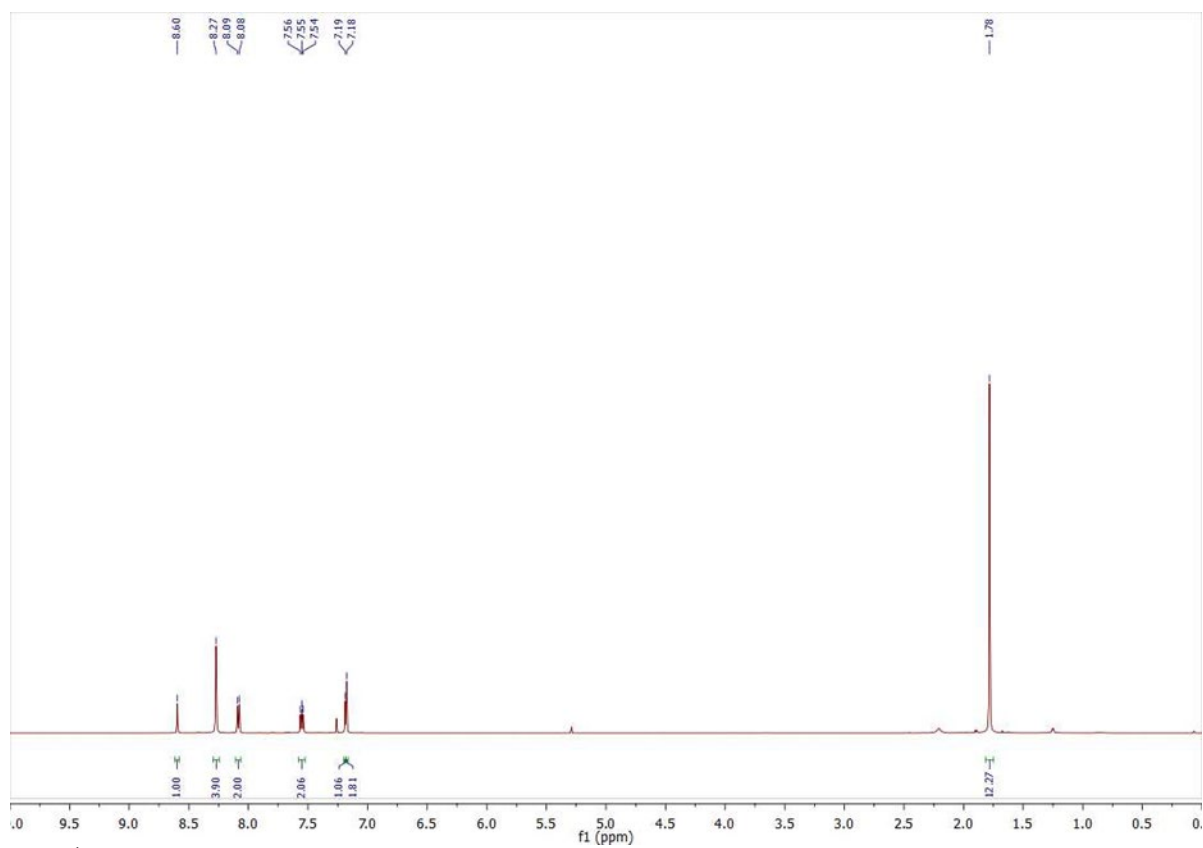


Figure S17.  $^1\text{H}$ -NMR spectrum of U1.

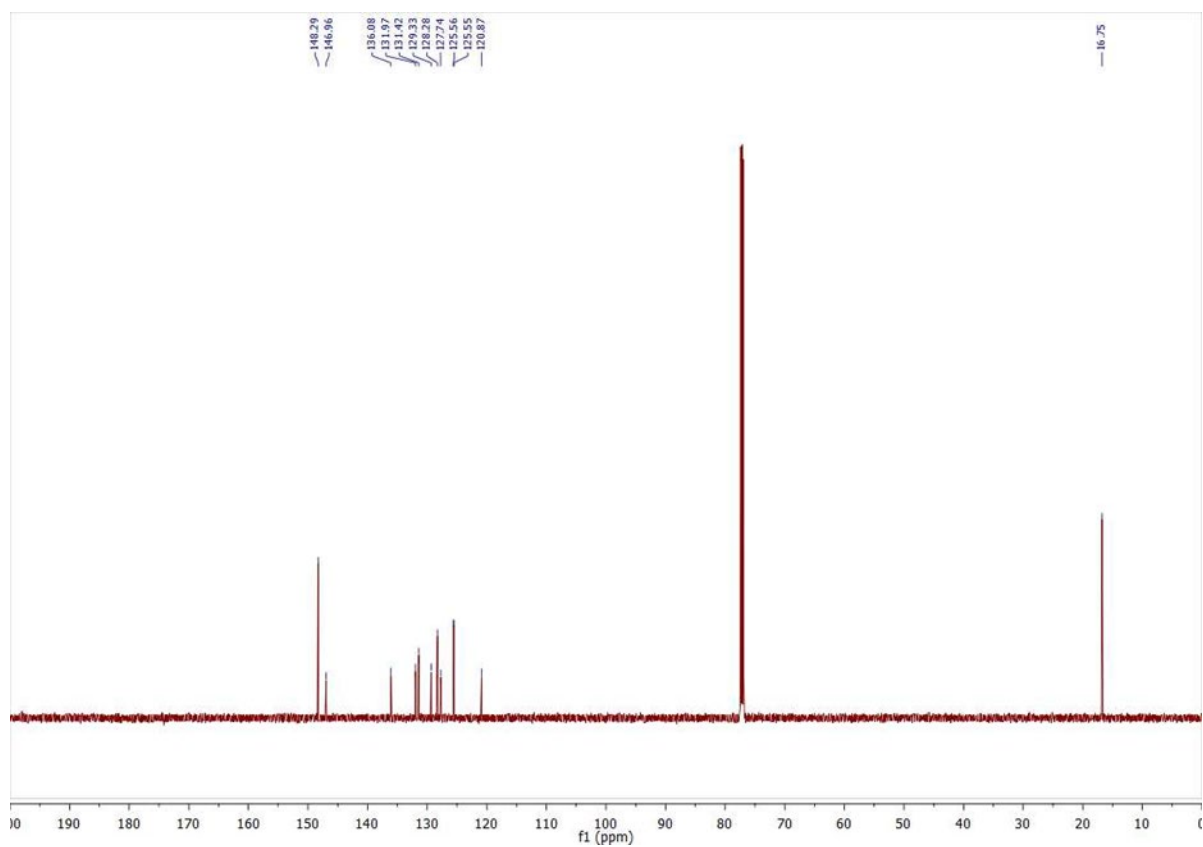


Figure S18.  $^{13}\text{C}\{^1\text{H}\}$ -NMR spectrum of U1.

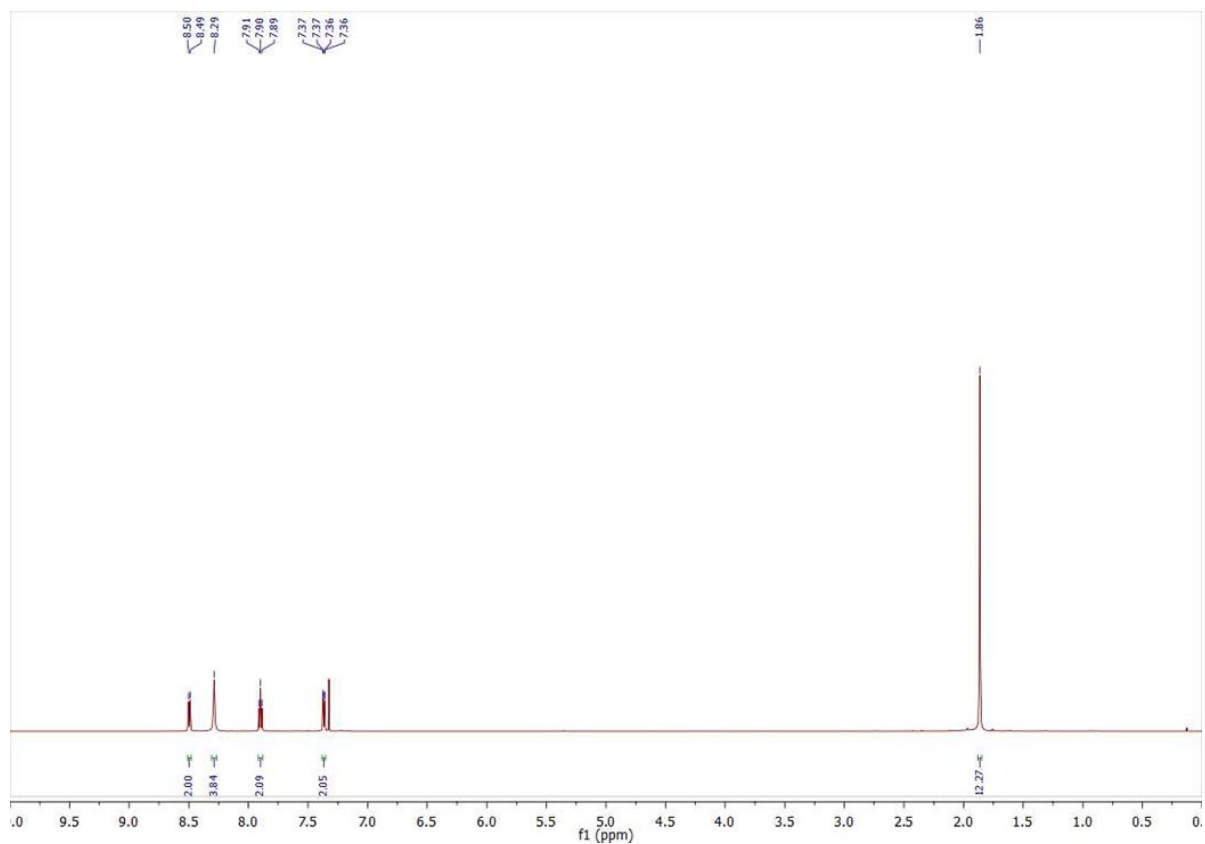


Figure S19.  $^1\text{H}$ -NMR spectrum of U2.

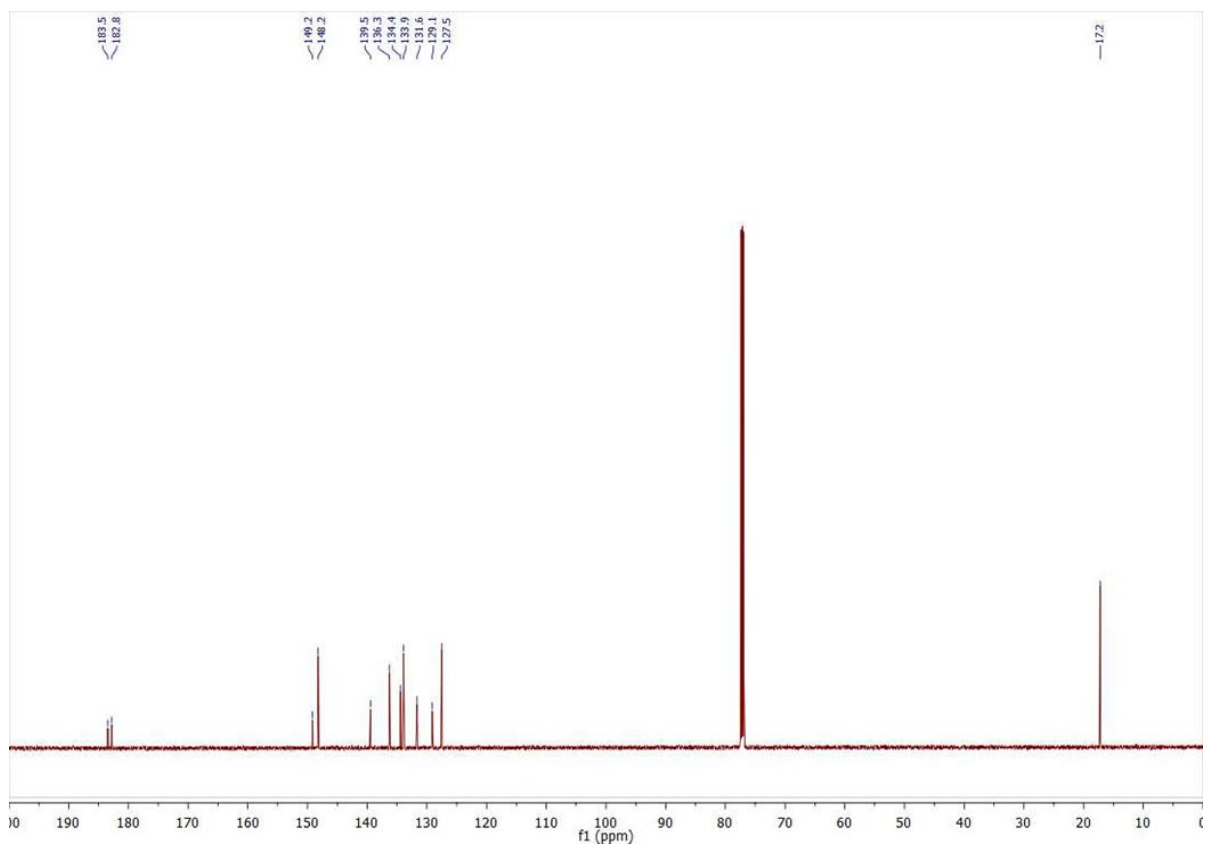


Figure S20.  $^{13}\text{C}\{^1\text{H}\}$ -NMR spectrum of U2.

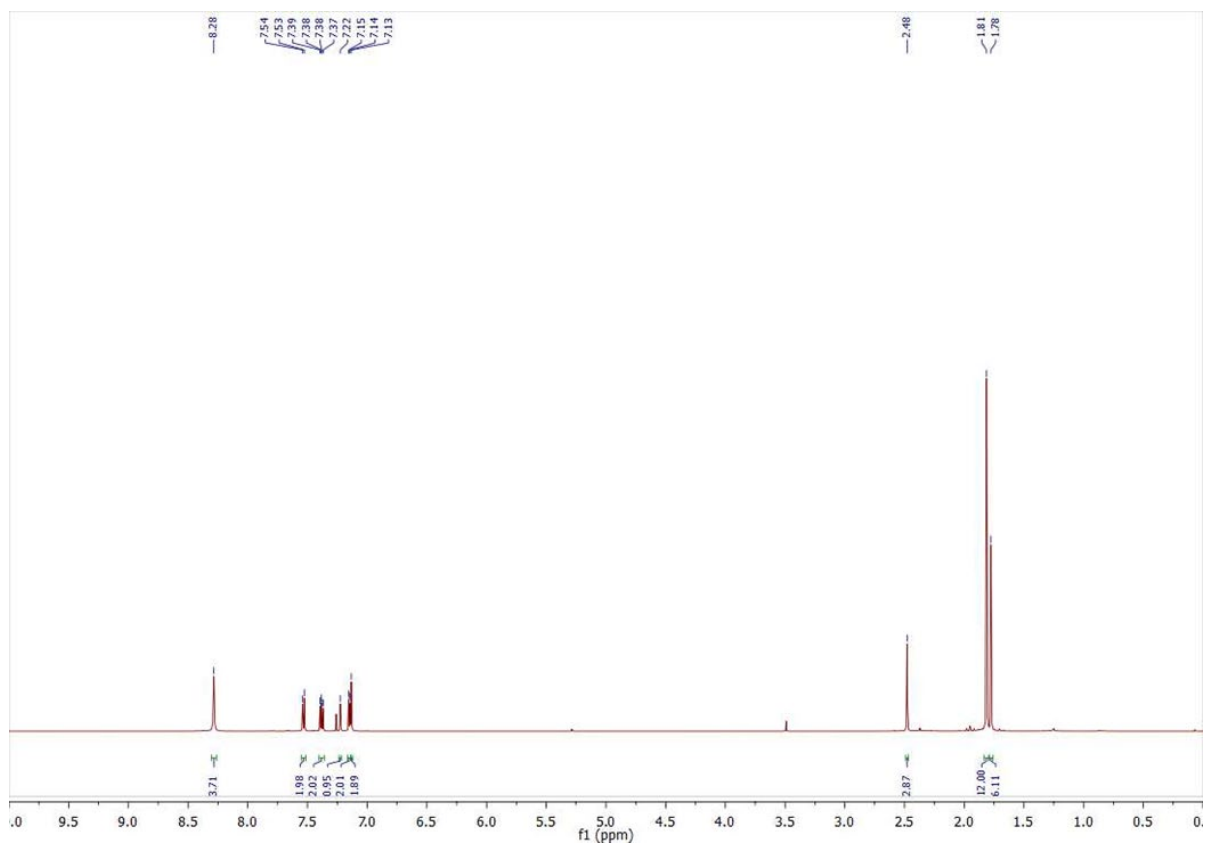


Figure S21.  $^1\text{H}$ -NMR spectrum of **U3**.

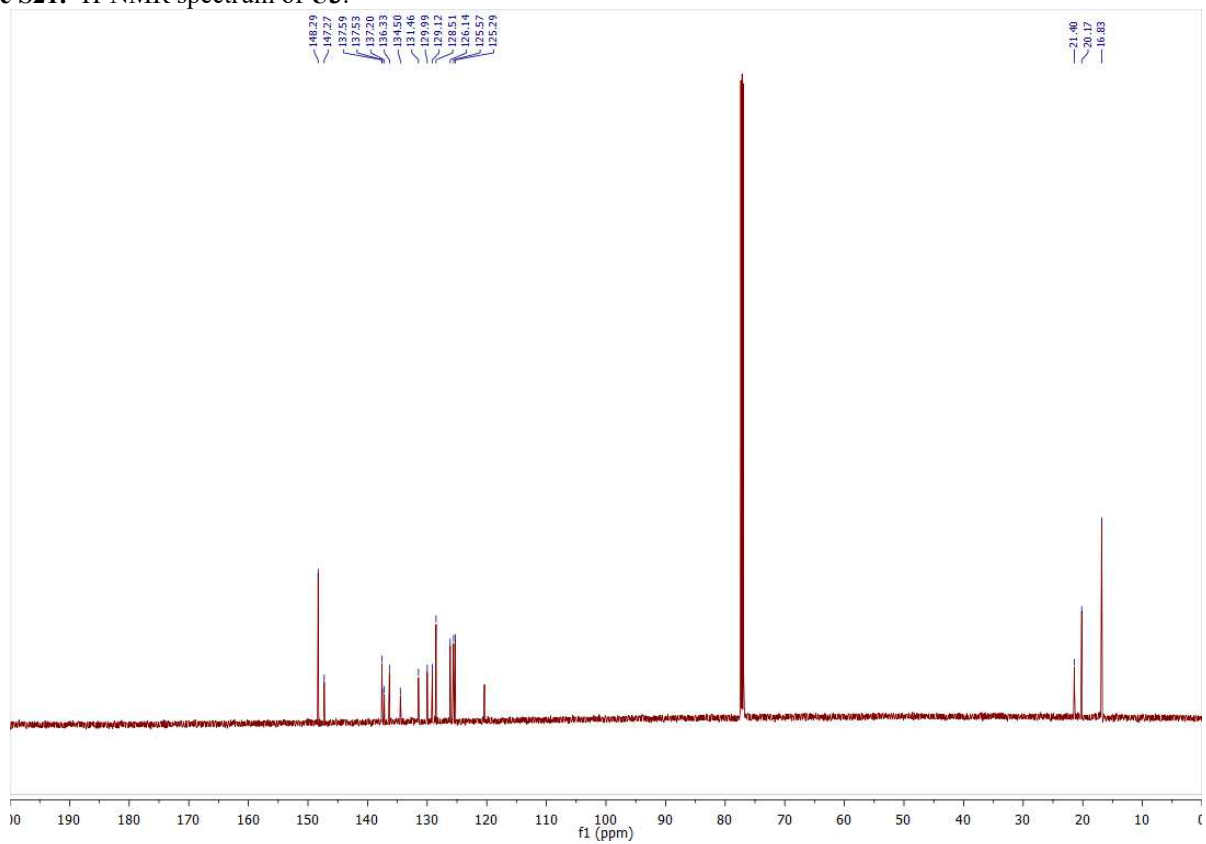


Figure S22.  $^{13}\text{C}\{^1\text{H}\}$ -NMR spectrum of **U3**.

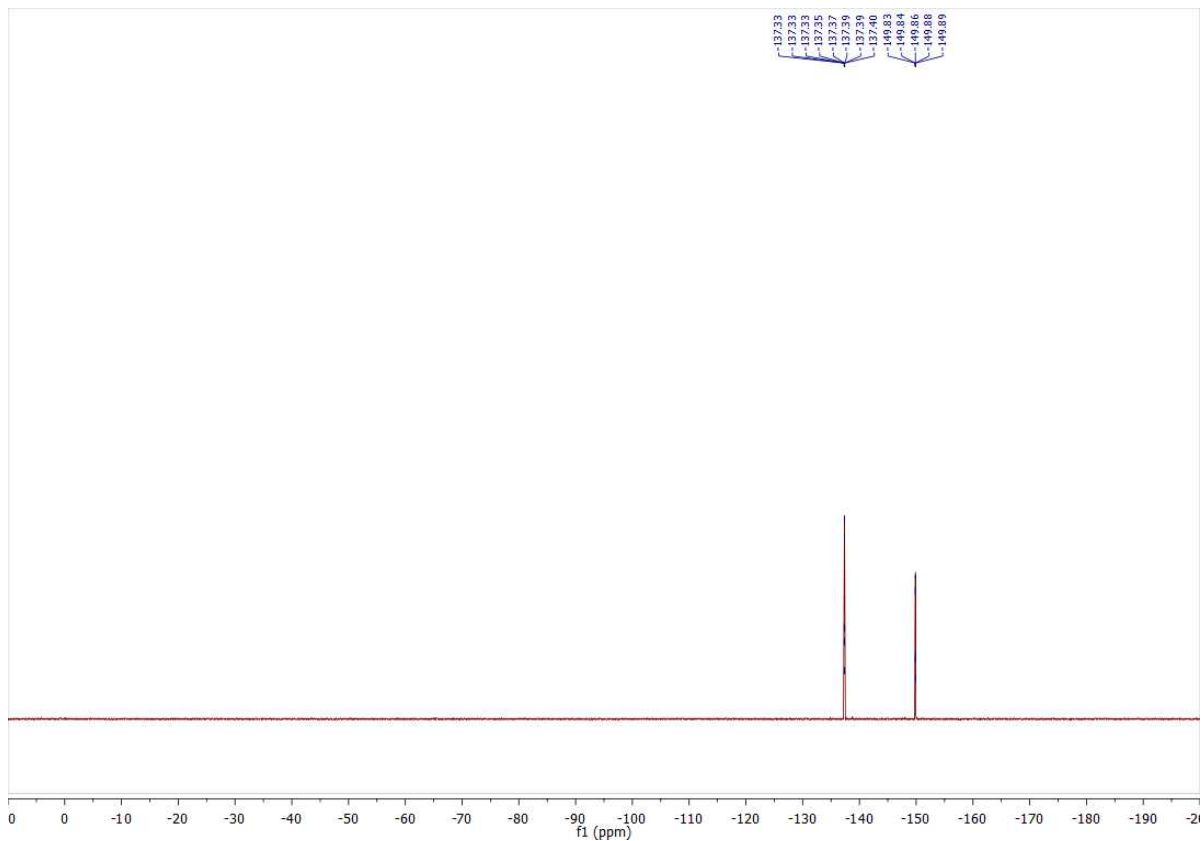


Figure S23.  $^{19}\text{F}$ -NMR spectrum of *E*-A2.

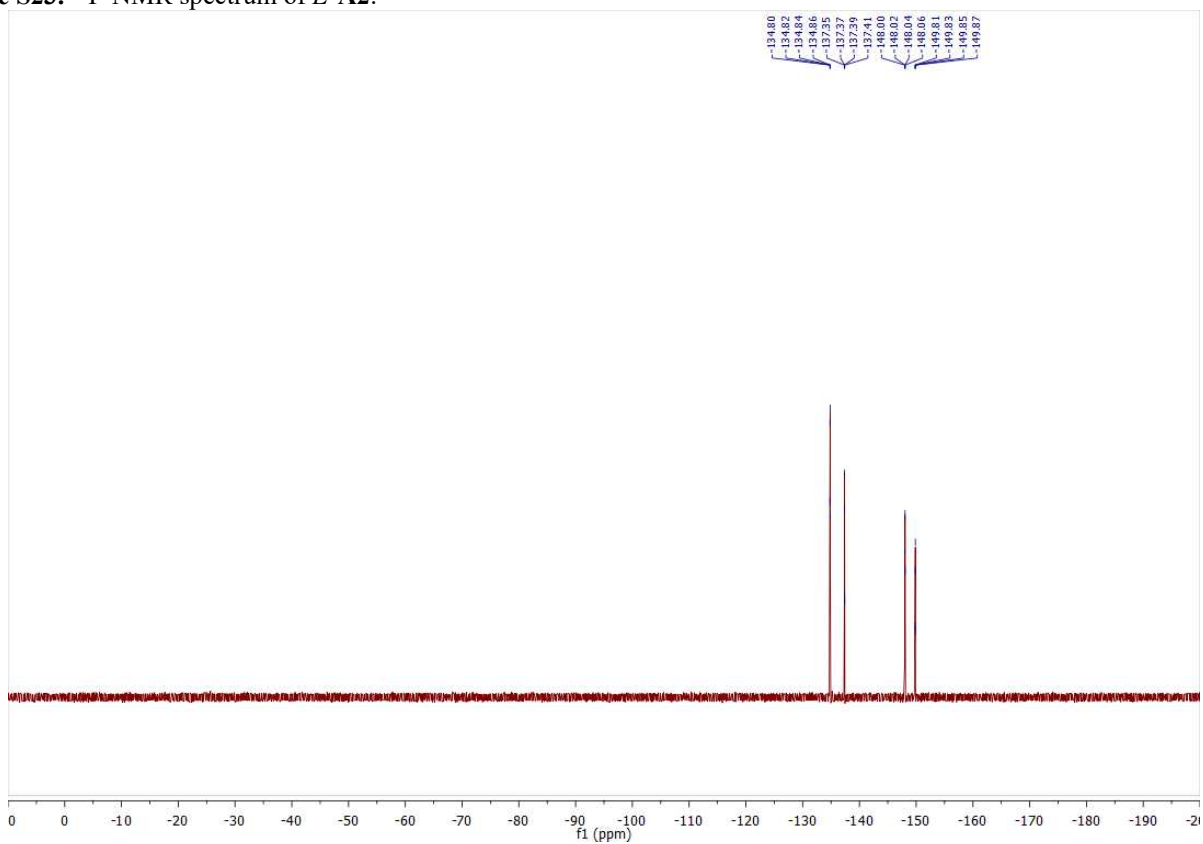


Figure S24.  $^{19}\text{F}$ -NMR spectrum of *E*-A2 and *Z*-A2.

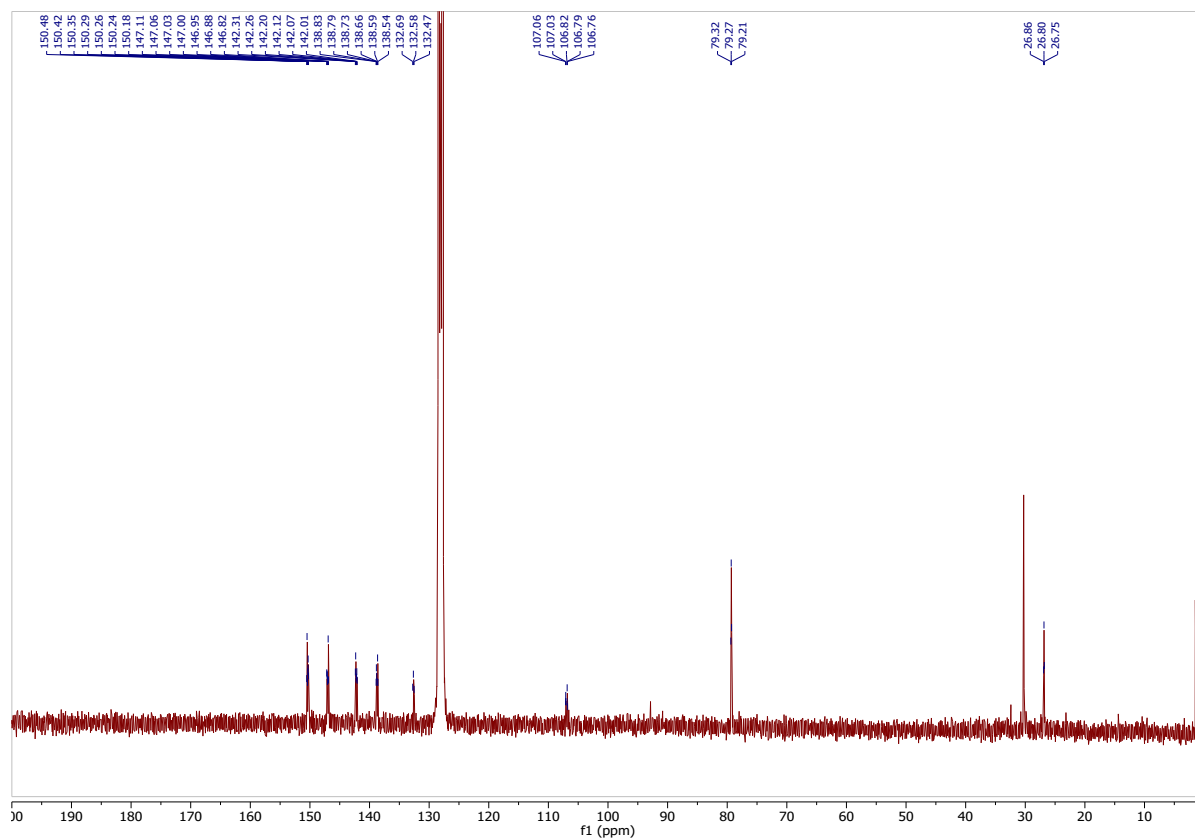


Figure S25.  $^{13}\text{C}\{^1\text{H}\}$ -NMR spectrum A2.